

Observation of $e^+e^- \rightarrow \omega\chi_{bJ}(1P)$ and search for $X_b \rightarrow \omega\Upsilon(1S)$ at \sqrt{s} near 10.75 GeV

I. Adachi , L. Aggarwal , H. Ahmed , H. Aihara , N. Akopov , A. Aloisio , N. Anh Ky , D. M. Asner , T. Aushev , V. Aushev , H. Bae , P. Bambade , Sw. Banerjee , J. Baudot , M. Bauer , A. Beaubien , J. Becker , P. K. Behera , J. V. Bennett , E. Bernieri , F. U. Bernlochner , V. Bertacchi , M. Bertemes , E. Bertholet , M. Bessner , S. Bettarini , B. Bhuyan , F. Bianchi , T. Bilka , D. Biswas , D. Bodrov , A. Bolz , J. Borah , A. Bozek , M. Bračko , P. Branchini , T. E. Browder , A. Budano , S. Bussino , M. Campajola , L. Cao , G. Casarosa , C. Cecchi , M.-C. Chang , P. Cheema , V. Chekelian , Y. Q. Chen , K. Chilikin , K. Chirapatpimol , H.-E. Cho , K. Cho , S.-J. Cho , S.-K. Choi , S. Choudhury , D. Cinabro , L. Corona , S. Cunliffe , S. Das , F. Dattola , E. De La Cruz-Burelo , S. A. De La Motte , G. De Nardo , M. De Nuccio , G. De Pietro , R. de Sangro , M. Destefanis , S. Dey , A. De Yta-Hernandez , R. Dhamija , A. Di Canto , F. Di Capua , Z. Doležal , I. Domínguez Jiménez , T. V. Dong , M. Dorigo , K. Dort , S. Dreyer , S. Dubey , G. Dujany , M. Eliachevitch , D. Epifanov , P. Feichtinger , T. Ferber , D. Ferlewicz , T. Fillinger , G. Finocchiaro , A. Fodor , F. Forti , B. G. Fulsom , E. Ganiev , V. Gaur , A. Gaz , A. Gellrich , G. Ghevondyan , R. Giordano , A. Giri , A. Glazov , B. Gobbo , R. Godang , P. Goldenzweig , S. Granderath , E. Graziani , D. Greenwald , Z. Gruberová , T. Gu , Y. Guan , K. Gudkova , J. Guilliams , T. Hara , K. Hayasaka , H. Hayashii , S. Hazra , C. Hearty , I. Heredia de la Cruz , M. Hernández Villanueva , A. Hershenhorn , T. Higuchi , E. C. Hill , H. Hirata , M. Hohmann , C.-L. Hsu , T. Iijima , K. Inami , G. Inguglia , N. Ipsita , A. Ishikawa , S. Ito , R. Itoh , M. Iwasaki , P. Jackson , W. W. Jacobs , D. E. Jaffe , E.-J. Jang , Q. P. Ji , S. Jia , Y. Jin , K. K. Joo , H. Junkerkalefeld , A. B. Kaliyar , K. H. Kang , R. Karl , G. Karyan , C. Ketter , C. Kiesling , C.-H. Kim , D. Y. Kim , K.-H. Kim , Y.-K. Kim , H. Kindo , P. Kodyš , T. Koga , S. Kohani , K. Kojima , T. Konno , A. Korobov , S. Korpar , E. Kovalenko , R. Kowalewski , T. M. G. Kraetzschmar , P. Križan , P. Krokovny , R. Kumar , K. Kumara , T. Kunigo , A. Kuzmin , Y.-J. Kwon , S. Lacaprara , T. Lam , L. Lanceri , J. S. Lange , M. Laurenza , K. Lautenbach , R. Leboucher , P. M. Lewis , C. Li , L. K. Li , J. Libby , K. Lieret , Z. Liptak , Q. Y. Liu , D. Liventsev , S. Longo , A. Lozar , T. Lueck , C. Lyu , M. Maggiora , R. Maiti , R. Manfredi , E. Manoni , S. Marcello , C. Marinas , L. Martel , A. Martini , T. Martinov , L. Massaccesi , M. Masuda , K. Matsuoka , S. K. Maurya , J. A. McKenna , M. Merola , F. Metzner , M. Milesi , C. Miller , K. Miyabayashi , R. Mizuk , N. Molina-Gonzalez , S. Moneta , H.-G. Moser , M. Mrvar , R. Mussa , I. Nakamura , M. Nakao , Y. Nakazawa , A. Narimani Charan , M. Naruki , Z. Natkaniec , A. Natochii , L. Nayak , M. Nayak , G. Nazaryan , N. K. Nisar , S. Ogawa , H. Ono , Y. Onuki , P. Oskin , A. Paladino , A. Panta , E. Paoloni , S. Pardi , H. Park , S.-H. Park , B. Paschen , A. Passeri , S. Paul , T. K. Pedlar , I. Peruzzi , R. Peschke , R. Pestotnik , M. Piccolo , L. E. Piilonen , P. L. M. Podesta-Lerma , T. Podobnik , S. Pokharel , L. Polat , C. Praz , S. Prell , E. Prencipe , M. T. Prim , H. Purwar , N. Rad , S. Raiz , A. Ramirez Morales , M. Reif , S. Reiter , M. Remnev , I. Ripp-Baudot , G. Rizzo , S. H. Robertson , J. M. Roney , A. Rostomyan , N. Rout , G. Russo , D. A. Sanders , S. Sandilya , A. Sangal , L. Santelj , Y. Sato , V. Savinov , B. Scavino , J. Schueler , C. Schwanda , Y. Seino , A. Selce , K. Senyo , J. Serrano , M. E. Sevir , C. Sfienti , C. P. Shen , X. D. Shi , T. Shillington , A. Sibidanov , J. B. Singh , J. Skorupa , R. J. Sobie , A. Soffer , E. Solovieva , S. Spataro , M. Starič , S. Stefkova , Z. S. Stottler , R. Stroili , Y. Sue , M. Sumihama , K. Sumisawa , W. Sutcliffe , S. Y. Suzuki , H. Svidras , M. Takizawa , U. Tamponi , K. Tanida , H. Tanigawa , F. Tenchini , A. Thaller , R. Tiwary , D. Tonelli , E. Torassa , N. Toutounji , K. Trabelsi , M. Uchida , I. Ueda , Y. Uematsu , T. Uglov , K. Unger , Y. Unno , K. Uno , S. Uno , Y. Ushiroda , S. E. Vahsen , R. van Tonder , G. S. Varner , A. Vinokurova , L. Vitale , V. Vobbiliseti , H. M. Wakeling , E. Wang , M.-Z. Wang , A. Warburton , S. Watanuki , M. Welsch , C. Wessel <

luminosity, respectively. These data were collected with the Belle II detector during special operations of the SuperKEKB collider above the $\Upsilon(4S)$ resonance. We report the first observation of $\omega\chi_{bJ}(1P)$ signals at $\sqrt{s} = 10.745$ GeV. By combining Belle II data with Belle results at $\sqrt{s} = 10.867$ GeV, we find energy dependencies of the Born cross sections for $e^+e^- \rightarrow \omega\chi_{b1,b2}(1P)$ to be consistent with the shape of the $\Upsilon(10753)$ state. These data indicate that the internal structures of the $\Upsilon(10753)$ and $\Upsilon(10860)$ states may differ. Including data at $\sqrt{s} = 10.653$ GeV, we also search for the bottomonium equivalent of the $X(3872)$ state decaying into $\omega\Upsilon(1S)$. No significant signal is observed for masses between 10.45 and 10.65 GeV/ c^2 .

Heavy quarkonium spectroscopy offers multiple opportunities for insight on the nonperturbative behavior of quantum chromodynamics [1–3]. Four bottomonium-like vector states have been identified above the $B\bar{B}$ threshold [4]. The $\Upsilon(10753)$, observed in $e^+e^- \rightarrow \pi^+\pi^-\Upsilon(nS)$ ($n = 1, 2, 3$) by Belle [5] and in fits to the $e^+e^- \rightarrow b\bar{b}$ cross sections at energies \sqrt{s} from 10.6 to 11.2 GeV [6], is particularly interesting.

The $\Upsilon(10753)$ has been interpreted as a conventional bottomonium [7–16], hybrid [17, 18], or tetraquark state [19–22]. Interpretations as an admixture of the conventional $4S$ and $3D$ states predict comparable branching fractions of 10^{-3} for $\Upsilon(10753) \rightarrow \pi^+\pi^-\Upsilon(nS)$ [7] and $\Upsilon(10753) \rightarrow \omega\chi_{bJ}$ [8], where χ_{bJ} denotes $\chi_{bJ}(1P)$ throughout. In this interpretation, the branching fraction for $\Upsilon(10753) \rightarrow \omega\chi_{b1}$ is expected to be about 1/5 of that for $\Upsilon(10753) \rightarrow \omega\chi_{b2}$ [8]. In addition, the process $e^+e^- \rightarrow \gamma X_b$, $X_b \rightarrow \omega\Upsilon(1S)$, which shares the same final states as $\Upsilon(10753) \rightarrow \omega\chi_{bJ}$, provides access to the X_b . The X_b is the posited bottomonium counterpart of the $X(3872)$ [23] ($\chi_{c1}(3872)$ [4]). Its existence has been predicted in molecular [24–34] and tetraquark models [35–38], with masses close to the $B\bar{B}^*$ threshold [24–34], or in the 10 to 11 GeV/ c^2 range [35–38], respectively. Unlike in $X(3872)$ decays, due to negligible isospin-breaking effects, the X_b may decay preferentially into $\pi^+\pi^-\pi^0\Upsilon(1S)$ instead of $\pi^+\pi^-\Upsilon(1S)$ [31–34]. Searches for an X_b state in $\pi^+\pi^-\Upsilon(1S)$ by CMS and ATLAS [39, 40], and in $e^+e^- \rightarrow \gamma X_b$, $X_b \rightarrow \pi^+\pi^-\pi^0\Upsilon(1S)$ near the $\Upsilon(10860)$ (known as the $\Upsilon(5S)$) energy by Belle [41], yielded null results.

In this Letter we test the nature of the $\Upsilon(10753)$ using measurements of Born cross sections for the $e^+e^- \rightarrow \omega\chi_{bJ}$ ($J = 0, 1, 2$) processes at \sqrt{s} between 10.701 and 10.805 GeV with $\omega \rightarrow \pi^+\pi^-\pi^0$, $\chi_{bJ} \rightarrow \gamma\Upsilon(1S)$, and $\Upsilon(1S) \rightarrow \ell^+\ell^-$ ($\ell = e$ or μ). We also search for the $X_b \rightarrow \omega\Upsilon(1S)$ process in $e^+e^- \rightarrow \gamma X_b$ at \sqrt{s} between 10.653 and 10.805 GeV. After event selection, fits to the two-dimensional invariant mass distributions for ω and χ_{bJ} candidates are used to search for $e^+e^- \rightarrow \omega\chi_{bJ}$ enhancements. Observed event yields as functions of collision energy are used to extract cross sections, which, combined with previous Belle measurements at higher energy, determine the energy dependence. Finally, $M(\omega\Upsilon(1S))$ invariant mass distributions are fitted to search for a X_b signal.

These analyses are based on electron-positron collisions produced by the SuperKEKB collider [42] at \sqrt{s}

= 10.653, 10.701, 10.745, and 10.805 GeV. Data samples, collected with the Belle II detector [43], correspond to integrated luminosities of 3.5, 1.6, 9.8, and 4.7 fb $^{-1}$ [44], respectively. The Belle II detector is a nearly 4π magnetic spectrometer surrounded by particle-identification detectors, an electromagnetic calorimeter, and muon and K_L^0 detectors [43]. Simulated events are used for optimization of event selections and determination of reconstruction efficiencies and resolution functions. We generate simulated signal events with EVTGEN [45]. Initial-state radiation (ISR) at next-to-leading order accuracy in quantum electrodynamics is simulated with PHOKHARA [46]. Angular distributions for the two-body decays in $e^+e^- \rightarrow \omega\chi_{bJ}$ and γX_b are generated according to a phase-space model. Simulated events are generated with varying X_b masses from 10.45 to 10.65 GeV/ c^2 [24–34]. The detector response is simulated with the Geant4 package [47]. Reconstruction of events from simulated and collision data is performed with the Belle II analysis software framework [48].

Events are selected online by a trigger [49] using central drift chamber and electromagnetic calorimeter information. In the offline analyses, all charged-particle trajectories (tracks) are required to originate from the vicinity of the interaction point. We require four or five tracks to reduce backgrounds while allowing for increased efficiency for signal events with an additional misreconstructed track. The identifications of pions, electrons, and muons are based on likelihood information from sub-detectors [50]. The pions are identified with 90% efficiency and 8% kaon contamination. At least one of the leptons is identified with 95% efficiency for electrons and 90% efficiency for muons. To reduce the effects of bremsstrahlung and final-state radiation, photons within a 50 mrad cone of the initial electron or positron direction are included in the calculation of the particle four-momentum. The $\Upsilon(1S)$ signal regions are selected as $9.25 < M(e^+e^-) < 9.58$ GeV/ c^2 and $9.34 < M(\mu^+\mu^-) < 9.58$ GeV/ c^2 .

Energy deposits in adjacent electromagnetic calorimeter crystals are treated as photon candidates if they are not associated with charged particles. We require the energy of the photon from the χ_{bJ} decay to exceed 50 MeV. Photons used to reconstruct π^0 candidates are required to have energies greater than 25, 25, and 40 MeV, when detected in the barrel, forward endcap, and backward endcap, respectively, and to satisfy $0.105 < M(\gamma\gamma) < 0.150$ GeV/ c^2 . We perform mass-constrained fits for the $\Upsilon(1S)$

and π^0 candidates to improve momentum resolutions.

We perform kinematic fits to the $\pi^+\pi^-\pi^0\gamma\Upsilon(1S)$ combinations constraining their four-momenta to the initial e^+e^- collision four-momentum. An average of 1.18 candidates per event is found in data. In events with multiple candidates, only the candidate with the smallest fit χ^2 is retained. To avoid systematic effects from the modeling of the beam-energy spread, we do not use the momenta after the kinematic fit.

Figure 1 shows distributions of $M(\gamma\Upsilon(1S))$ and $M(\pi^+\pi^-\pi^0)$ for events restricted to $9.75 < M(\gamma\Upsilon(1S)) < 10$ GeV/ c^2 and $0.61 < M(\pi^+\pi^-\pi^0) < 0.95$ GeV/ c^2 , where signals are clearly visible at $\sqrt{s} = 10.745$ and 10.805 GeV.

We perform a two-dimensional unbinned likelihood fit to the $M(\gamma\Upsilon(1S))$ versus $M(\pi^+\pi^-\pi^0)$ distributions for data collected at $\sqrt{s} = 10.745$ and 10.805 GeV [51]. The fit function is a sum of four components: signals in $M(\gamma\Upsilon(1S))$ and $M(\pi^+\pi^-\pi^0)$ distributions, peaking background in the $M(\gamma\Upsilon(1S))$ distribution from $e^+e^- \rightarrow \pi^+\pi^-\pi^0\chi_{bJ}$, peaking background in the $M(\pi^+\pi^-\pi^0)$ distribution from non- χ_{bJ} backgrounds with a ω , and combinatorial background. Each χ_{bJ} signal shape is described by a Crystal Ball function [52] while the ω signal shape is described by a Breit-Wigner function (BW) convolved with a Gaussian function. The widths of the Crystal Ball and Gaussian functions are approximately 15 MeV/ c^2 and 13 MeV/ c^2 , respectively. Signal shape parameters are fixed from a fit to simulated signal events. A product of linear functions is used to describe the combinatorial background.

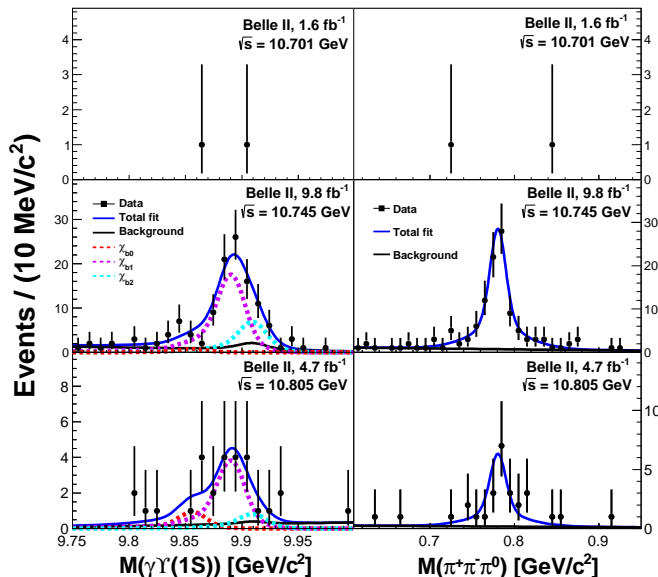


FIG. 1: Distributions of (left) $\gamma\Upsilon(1S)$ and (right) $\pi^+\pi^-\pi^0$ masses in data at $\sqrt{s} = 10.701$, 10.745, and 10.805 GeV with fit results overlaid.

Fit results are presented in Table I. We find significant signals of χ_{b1} and χ_{b2} at $\sqrt{s} = 10.745$ GeV. The signif-

icances of the χ_{b0} , χ_{b1} , and χ_{b2} signals at 10.745 GeV and 10.805 GeV are 11σ and 4.5σ , respectively. We report the first observation of $\omega\chi_{bJ}$ signals at $\sqrt{s} = 10.745$ GeV. These significances are estimated using Wilks' theorem [53]. We compute 90% Bayesian credibility upper limits on the yields assuming uniform priors (Table I). Systematic uncertainties in the Born cross-section measurements (discussed below) are approximately included by convolving the likelihood with a Gaussian function whose width equals the total systematic uncertainty.

For data collected at $\sqrt{s} = 10.701$ GeV, the signal yield is calculated as $N^{\text{sig}} = \max(0, N^{\text{obs}} - N^b)$. The observed yield N^{obs} is obtained by counting events in the χ_{b0} , χ_{b1} , and χ_{b2} signal regions of $9.80 < M(\gamma\Upsilon(1S)) < 9.89$ GeV/ c^2 , $9.84 < M(\gamma\Upsilon(1S)) < 9.93$ GeV/ c^2 , and $9.86 < M(\gamma\Upsilon(1S)) < 9.95$ GeV/ c^2 , respectively, in which about 95% of signal candidates are retained; the background yields N^b in the χ_{bJ} signal regions are obtained by scaling background events with the luminosity using $\sqrt{s} = 10.745$ GeV data. The statistical uncertainty for N^{sig} is estimated using a Bayesian approach including background uncertainties [54]. The upper limit at 90% Bayesian credibility on N^{sig} (N^{UL}) is also determined with the same approach. Signal yields and upper limits are listed in Table I.

The $e^+e^- \rightarrow \omega\chi_{bJ}$ Born cross section is calculated using

$$\sigma_B(e^+e^- \rightarrow \omega\chi_{bJ}) = \frac{N^{\text{sig}} |1 - \Pi|^2}{\mathcal{L} \varepsilon \mathcal{B}_{\text{int}} (1 + \delta_{\text{ISR}})}, \quad (1)$$

where \mathcal{L} is the integrated luminosity, ε is the reconstruction efficiency, \mathcal{B}_{int} is the product of the branching fractions of the intermediate states, $|1 - \Pi|^2$ is the vacuum polarization factor [6, 55], and $(1 + \delta_{\text{ISR}})$ is the radiative-correction factor [56–58]. In calculating the radiative-correction factor, we use the energy dependence of the Born cross sections measured in this work. Values of the inputs, resulting Born cross sections, and their upper limits for non-significant signals are listed in Table I.

Combining $\sigma_B(e^+e^- \rightarrow \omega\chi_{b1} \text{ and } \omega\chi_{b2}) = (0.76 \pm 0.16)$ and (0.29 ± 0.14) pb at $\sqrt{s} = 10.867$ GeV from Belle [41] and those from this work, we show the Born cross sections for $e^+e^- \rightarrow \omega\chi_{b1}$ and $\omega\chi_{b2}$ as functions of collision energy in Fig. 2. We observe a strong enhancement of the cross section near 10.75 GeV. We fit these distributions with a coherent sum of a two-body phase-space and a BW function [59]

$$|\sqrt{\Phi_2(\sqrt{s})} + \frac{\sqrt{12\pi\Gamma_{ee}\mathcal{B}_f\Gamma}}{s - M^2 - iM\Gamma} \sqrt{\frac{\Phi_2(\sqrt{s})}{\Phi_2(M)}} e^{i\phi}|^2, \quad (2)$$

where M is the mass of the $\Upsilon(10753)$, Γ (Γ_{ee}) is its total (electron) width, \mathcal{B}_f is the branching fraction for the decay $\Upsilon(10753) \rightarrow \omega\chi_{b1}$ or $\omega\chi_{b2}$, Φ_2 is the two-body phase-space factor, and ϕ is the relative phase between the amplitudes. In the fits, the mass and total width in the BW function are fixed to 10752.7 MeV/ c^2 and

TABLE I: Measurements of $e^+e^- \rightarrow \omega\chi_{bJ}$ at $\sqrt{s} = 10.701, 10.745, \text{ and } 10.805$ GeV. Σ is the signal significance; Syst is the systematic uncertainty. The first and second uncertainties (if available) indicate statistical and systematic contributions, respectively. The common systematic uncertainties for all energy points are 15.8%, 9.4%, and 9.3% for $\omega\chi_{b0}, \omega\chi_{b1}, \text{ and } \omega\chi_{b2}$, respectively.

Channel	\sqrt{s} (GeV)	N^{sig}	N^{UL}	$\Sigma(\sigma)$	ε	$ 1 - \Pi ^2$	$1 + \delta_{\text{ISR}}$	Syst (%)	σ_B (pb)	σ_B^{UL} (pb)
$e^+e^- \rightarrow \omega\chi_{b0}$	10.701	$0.0_{-0.0}^{+1.1}$	3.0	-	0.182	0.931	0.67	16.6	$0.0_{-0.0}^{+6.1}$	16.6
$e^+e^- \rightarrow \omega\chi_{b1}$		$0.0_{-0.0}^{+2.1}$	3.9	-	0.184	0.931	0.64	10.6	$0.0_{-0.0}^{+0.7}$	1.2
$e^+e^- \rightarrow \omega\chi_{b2}$		$0.1_{-0.1}^{+2.2}$	4.0	-	0.182	0.931	0.62	10.6	$0.1_{-0.1}^{+1.4}$	2.5
$e^+e^- \rightarrow \omega\chi_{b0}$	10.745	$3.0_{-4.7}^{+5.5}$	12.0	0.5	0.183	0.931	0.65	25.9	$2.8_{-4.4}^{+5.1} \pm 0.7$	11.3
$e^+e^- \rightarrow \omega\chi_{b1}$		$68.9_{-13.5}^{+13.7}$	-	5.9	0.183	0.931	0.65	12.7	$3.6_{-0.7}^{+0.7} \pm 0.5$	-
$e^+e^- \rightarrow \omega\chi_{b2}$		$27.6_{-10.0}^{+11.6}$	-	3.1	0.184	0.931	0.65	14.5	$2.8_{-1.0}^{+1.2} \pm 0.4$	-
$e^+e^- \rightarrow \omega\chi_{b0}$	10.805	$3.6_{-3.1}^{+3.8}$	9.9	1.2	0.182	0.932	1.12	24.9	$4.1_{-3.5}^{+4.3} \pm 1.0$	11.4
$e^+e^- \rightarrow \omega\chi_{b1}$		$15.0_{-6.2}^{+6.8}$	26.2	2.7	0.182	0.932	1.12	20.2	$0.9_{-0.4}^{+0.4} \pm 0.2$	1.7
$e^+e^- \rightarrow \omega\chi_{b2}$		$3.3_{-3.8}^{+5.3}$	12.8	0.8	0.183	0.932	1.11	29.1	$0.4_{-0.5}^{+0.7} \pm 0.1$	1.6

35.5 MeV [5], respectively. There are two solutions for $\Gamma_{ee}\mathcal{B}(\Upsilon(10753) \rightarrow \omega\chi_{b1} \text{ and } \omega\chi_{b2})$. One corresponds to constructive interference and yields $(0.63 \pm 0.39(\text{stat}) \pm 0.20(\text{syst}))$ and $(0.53 \pm 0.46(\text{stat}) \pm 0.15(\text{syst}))$ eV (Solution I). The other corresponds to destructive interference and yields $(2.01 \pm 0.38(\text{stat}) \pm 0.76(\text{syst}))$ and $(1.32 \pm 0.44(\text{stat}) \pm 0.55(\text{syst}))$ eV (Solution II). The systematic uncertainties are discussed below. The fit qualities for $\omega\chi_{b1}$ and $\omega\chi_{b2}$ are $\chi^2/\text{ndf} = 0.5/1$ and $0.1/1$. An alternative model with two interfering BW functions for the $\Upsilon(10753)$ and $\Upsilon(10860)$ states shows little interference and $\Gamma_{ee}\mathcal{B}(\Upsilon(10753) \rightarrow \omega\chi_{b1} \text{ and } \omega\chi_{b2}) = (1.24 \pm 0.56(\text{stat}))$ and $(0.92 \pm 0.37(\text{stat}))$ eV (Solution I) and $(1.28 \pm 0.57(\text{stat}))$ and $(1.09 \pm 0.40(\text{stat}))$ eV (Solution II). The fit qualities for $\omega\chi_{b1}$ and $\omega\chi_{b2}$ are $\chi^2/\text{ndf} = 0.4/1$ and $0.1/1$. We also test a single BW of $\Upsilon(10753)$ with a free mass and width to fit the energy dependence, and find a less satisfactory χ^2/ndf of 12/6.

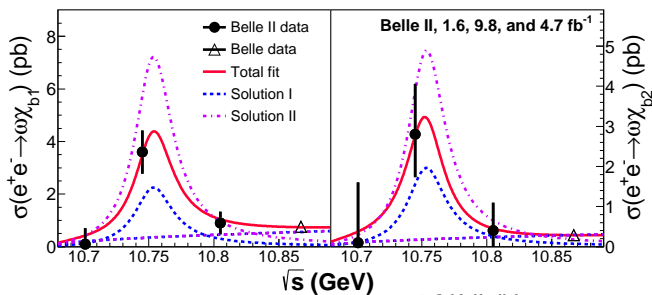


FIG. 2: Energy dependence of the Born cross sections for (left) $e^+e^- \rightarrow \omega\chi_{b1}$ and (right) $e^+e^- \rightarrow \omega\chi_{b2}$. Circles show the measurements reported here, triangles are the results of the Belle experiment [41]. Error bars represent combined statistical and systematic uncertainties. Curves show the fit results and various components of the fit function.

In addition, we search for the X_b in $e^+e^- \rightarrow \gamma X_b$ with $X_b \rightarrow \omega\Upsilon(1S)$ at $\sqrt{s} = 10.653, 10.701, 10.745, \text{ and } 10.805$ GeV. Distributions of $M(\omega\Upsilon(1S))$ for events

within $0.70 < M(\pi^+\pi^-\pi^0) < 0.86$ GeV/ c^2 are shown in Fig. 3. Prominent reflections of $e^+e^- \rightarrow \omega\chi_{bJ}$ signals are observed, but no narrow structure as expected from a X_b signal is found. We set upper limits at 90% Bayesian credibility [54] with $M(\omega\Upsilon(1S))$ in the 100 MeV/ c^2 interval centered at the test X_b mass (95% signal efficiency). The observed yield is obtained by counting events, and the background yield is estimated using an unbinned maximum likelihood fit to the $M(\omega\Upsilon(1S))$ distribution. A straight line is used to describe the smooth background. At $\sqrt{s} = 10.701, 10.745, \text{ and } 10.805$ GeV, additional normalized shapes from simulations for each χ_{bJ} state are used to describe $e^+e^- \rightarrow \omega\chi_{bJ}$ signals.

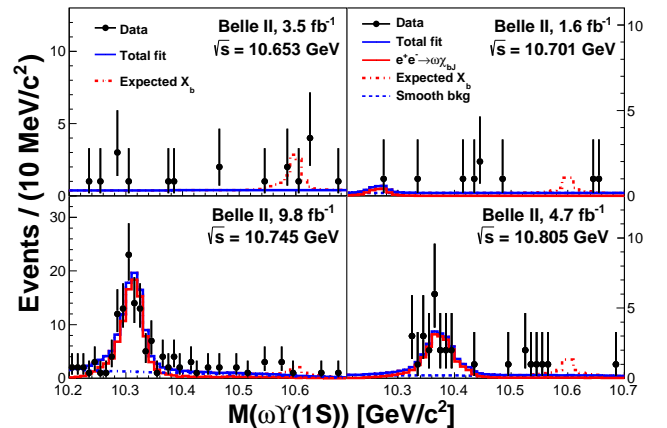


FIG. 3: Distributions of $\omega\Upsilon(1S)$ mass from data at $\sqrt{s} = 10.653, 10.701, 10.745, \text{ and } 10.805$ GeV. The red dash-dotted histograms are from simulated events $e^+e^- \rightarrow \gamma X_b (\rightarrow \omega\Upsilon(1S))$ with the X_b mass fixed at 10.6 GeV/ c^2 and yields fixed at the upper limit values.

We calculate the upper limits at 90% Bayesian credibility on the products of the Born cross section for the $e^+e^- \rightarrow \gamma X_b$ process and the branching fraction for $X_b \rightarrow \omega\Upsilon(1S)$ ($\sigma_B^{\text{UL}}(e^+e^- \rightarrow \gamma X_b)\mathcal{B}(X_b \rightarrow \omega\Upsilon(1S))$)

with varying X_b masses from 10.45 to 10.65 GeV/ c^2 using a similar relationship as Eq. (1). The least stringent limits on signal yields are 10.0, 8.1, 8.1, 10.7 with $m(X_b) = 10.59, 10.45, 10.45, \text{ and } 10.53$ GeV/ c^2 at $\sqrt{s} = 10.653, 10.701, 10.745, 10.805$ GeV, respectively, with an efficiency of about 16%. The values of $\sigma_B^{\text{UL}}(e^+e^- \rightarrow \gamma X_b)\mathcal{B}(X_b \rightarrow \omega\Upsilon(1S))$ range in (0.14 – 0.55) pb, (0.25 – 0.84) pb, (0.06 – 0.14) pb, and (0.08 – 0.37) pb, respectively [60].

The individual sources of systematic uncertainties considered in the measurements of $\sigma_B(e^+e^- \rightarrow \omega\chi_{bJ})$ and $\sigma_B(e^+e^- \rightarrow \gamma X_b)\mathcal{B}(X_b \rightarrow \omega\Upsilon(1S))$ are listed in the Supplemental Material [61] and the total systematic uncertainties are listed in Table I. Detection efficiency uncertainties include momentum-dependent tracking uncertainties (1.3% per pion and 0.3% per lepton, as derived from $\bar{B}^0 \rightarrow D^{*+}(\rightarrow D^0\pi^+)\pi^-$ and $e^+e^- \rightarrow \tau^+\tau^-$), particle identification (1.1% per pion, as derived from $D^{*+} \rightarrow D^0(\rightarrow K^-\pi^+)\pi^+$), lepton identification (0.4% per electron and 0.7% per muon, as derived from J/ψ decays, Bhabha, dimuon, and two-photon processes), photon reconstruction (3.5% per photon, as derived from $e^+e^- \rightarrow \gamma\mu^+\mu^-$), and π^0 reconstruction (4.8% per π^0 , as derived from $\eta \rightarrow \pi^0\pi^0\pi^0$). The uncertainties on the branching fractions, 14.7%, 7.4%, and 7.3% for $\chi_{b0}, \chi_{b1}, \text{ and } \chi_{b2}$ decays, are taken from Ref. [4]. For $\sigma_B(e^+e^- \rightarrow \omega\chi_{bJ})$, we change the mass and width values of $\Upsilon(10753)$ by one standard deviation [5], and the fit model from the coherent sum of a two-body phase-space and a BW function to two interfering BW functions for the $\Upsilon(10753)$ and $\Upsilon(10860)$. The differences on the radiative correction factors are 2.0%, 5.1%, and 13.7% for $\sqrt{s} = 10.701, 10.745, \text{ and } 10.805$ GeV, respectively. We assume $\sigma(e^+e^- \rightarrow \gamma X_b)$ to be proportional to $1/s^2$ to determine the radiative-correction factor for $e^+e^- \rightarrow \gamma X_b$. The maximum difference on the radiative-correction factor observed by using $1/s$ or $1/s^3$ is included as an uncertainty, which is less than 1%. The uncertainty associated with the assumption of uniform distribution for the $\omega\chi_{bJ}$ (or γX_b) particles is assessed by using an alternative signal efficiency based on a $1 \pm \cos^2\theta$ distribution, where θ is the ω (γ) angle in e^+e^- center-of-mass frame. For $\sigma_B(e^+e^- \rightarrow \omega\chi_{bJ})$ at $\sqrt{s} = 10.745$ and 10.805 GeV, we estimate the systematic uncertainties associated with the fit by changing the order of the background polynomial and the range of the fit, and comparing the fit results without a χ_{b0} component. The resulting systematic uncertainties are 16.3%, 4.6%, 8.2% and 10.9%, 8.9%, 20.0% for $\chi_{b0,b1,b2}$ decays at $\sqrt{s} = 10.745$ and 10.805 GeV. Studies in the control channel $e^+e^- \rightarrow \pi^+\pi^+\pi^-\pi^-\pi^0\pi^0$ show that a 1% uncertainty needs to be included due to mismodeling in the trigger simulation. We assume a beam-energy calibration uncertainty of 5 MeV and take the fractional differences in signal yields as uncertainties. These are 10.5%, 2.5%, 3.0% and 6.5%, 5.0%, 12.2% for $\chi_{b0,b1,b2}$ decays at $\sqrt{s} = 10.745$ and 10.805 GeV. Belle II measures the luminosity at a 0.6% precision [44]. Systematic uncertainties on the

$\Gamma_{ee}\mathcal{B}(\Upsilon(10753) \rightarrow \omega\chi_{b1} \text{ and } \omega\chi_{b2})$ determination come from variations of the $\Upsilon(10753)$ parameters and collision energies within their uncertainties.

In summary, we use a unique sample of electron-positron data collected at center-of-mass energies between 10.653 and 10.805 GeV to measure the Born cross sections for the $e^+e^- \rightarrow \omega\chi_{bJ}$ process and search for the X_b state decaying into $\omega\Upsilon(1S)$. A significant $\omega\chi_{b1}$ signal and evidence for the $e^+e^- \rightarrow \omega\chi_{b2}$ process at $\sqrt{s} = 10.745$ GeV are found. The corresponding Born cross sections are $(3.6_{-0.7}^{+0.7}(\text{stat}) \pm 0.5(\text{syst}))$ pb and $(2.8_{-1.0}^{+1.2}(\text{stat}) \pm 0.4(\text{syst}))$ pb. We observe a strong enhancement of the cross section near 10.75 GeV whose energy dependence is consistent with the $\Upsilon(10753)$ state. We measure the products $\Gamma_{ee}\mathcal{B}(\Upsilon(10753) \rightarrow \omega\chi_{b1} \text{ and } \omega\chi_{b2})$ to be in the range 0.20–2.9 and 0.05–2.0 eV.

The observed ratio $\sigma_B(e^+e^- \rightarrow \omega\chi_{b1})/\sigma_B(e^+e^- \rightarrow \omega\chi_{b2}) = 1.3 \pm 0.6$ at $\sqrt{s} = 10.745$ GeV, where the statistical uncertainties and all the uncommon systematic uncertainties are included, contradicts the expectation for a pure D -wave bottomonium state of 15 [62, 63]. There is also a 1.8σ difference with the prediction for a $S - D$ -mixed state of 0.2 [8].

This analysis shows that the $e^+e^- \rightarrow \omega\chi_{bJ}$ process observed near $\Upsilon(10860)$ by Belle could be due to the tail of the $\Upsilon(10753)$. The large difference between the small value of the $\omega\chi_{bJ}$ to $\pi^+\pi^-\Upsilon(nS)$ production rate at the $\Upsilon(10860)$ and the value at the $\Upsilon(10753)$ may indicate different internal structures for these two states, which otherwise have the same quantum numbers and are only 110 MeV/ c^2 apart.

No evidence of a X_b signal is obtained for X_b masses between 10.45 and 10.65 GeV/ c^2 , and upper limits at 90% Bayesian credibility on the products of Born cross section for $e^+e^- \rightarrow \gamma X_b$ and branching fraction for $X_b \rightarrow \omega\Upsilon(1S)$ are set to be 0.55, 0.84, 0.14, and 0.37 pb at $\sqrt{s} = 10.653, 10.701, 10.745, \text{ and } 10.805$ GeV, respectively.

We warmly thank Fengkun Guo, Xiang Liu, Di-anyong Chen, and Zhiyong Zhou for valuable and helpful discussions. This work, based on data collected using the Belle II detector, which was built and commissioned prior to March 2019, was supported by Science Committee of the Republic of Armenia Grant No. 20TTCG-1C010; Australian Research Council and research Grants No. DE220100462, No. DP180102629, No. DP170102389, No. DP170102204, No. DP150103061, No. FT130100303, No. FT130100018, and No. FT120100745; Austrian Federal Ministry of Education, Science and Research, Austrian Science Fund No. P 31361-N36 and No. J4625-N, and Horizon 2020 ERC Starting Grant No. 947006 ‘‘InterLeptons’’; Natural Sciences and Engineering Research Council of Canada, Compute Canada and CANARIE; Chinese Academy of Sciences and research Grant No. QYZDJ-SSW-SLH011, National Natural Science Foundation of

China and research Grants No. 11521505, No. 11575017, No. 11675166, No. 11761141009, No. 11705209, and No. 11975076, Liaoning Revitalization Talents Program under Contract No. XLYC1807135, Shanghai Municipal Science and Technology Committee under Contract No. 19ZR1403000, Shanghai Pujiang Program under Grant No. 18PJ1401000, and the CAS Center for Excellence in Particle Physics (CCEPP); the Ministry of Education, Youth, and Sports of the Czech Republic under Contract No. LTT17020 and Charles University Grant No. SVV 260448 and the Czech Science Foundation Grant No. 22-18469S; European Research Council, Seventh Framework PIEF-GA-2013-622527, Horizon 2020 ERC-Advanced Grants No. 267104 and No. 884719, Horizon 2020 ERC-Consolidator Grant No. 819127, Horizon 2020 Marie Skłodowska-Curie Grant Agreement No. 700525 "NIOBE" and No. 101026516, and Horizon 2020 Marie Skłodowska-Curie RISE project JENNIFER2 Grant Agreement No. 822070 (European grants); L'Institut National de Physique Nucléaire et de Physique des Particules (IN2P3) du CNRS (France); BMBF, DFG, HGF, MPG, and AvH Foundation (Germany); Department of Atomic Energy under Project Identification No. RTI 4002 and Department of Science and Technology (India); Israel Science Foundation Grant No. 2476/17, U.S.-Israel Binational Science Foundation Grant No. 2016113, and Israel Ministry of Science Grant No. 3-16543; Istituto Nazionale di Fisica Nucleare and the research grants BELLE2; Japan Society for the Promotion of Science, Grant-in-Aid for Scientific Research Grants No. 16H03968, No. 16H03993, No. 16H06492, No. 16K05323, No. 17H01133, No. 17H05405, No. 18K03621, No. 18H03710, No. 18H05226, No. 19H00682, No. 22H00144, No. 26220706, and No. 26400255, the National Institute of Informatics, and Science Information NETWORK 5 (SINET5), and the Ministry of Education, Culture, Sports, Science, and Technology (MEXT) of Japan; National Research Foundation (NRF) of Korea Grants No. 2016R1D1A1B-02012900, No. 2018R1A2B3003643, No. 2018R1A6A1A-06024970, No. 2018R1D1A1B07047294, No. 2019K1-A3A7A09033840, No. 2019R1I1A3A01058933, and No. 2022R1A2C1003993, Radiation Science Research Institute, Foreign Large-size Research Facility Application Supporting project, the Global Science Experimental Data Hub Center of the Korea Institute of Science and Technology Information and KREONET/GLORIAD;

Universiti Malaya RU grant, Akademi Sains Malaysia, and Ministry of Education Malaysia; Frontiers of Science Program Contracts No. FOINS-296, No. CB-221329, No. CB-236394, No. CB-254409, and No. CB-180023, and No. SEP-CINVESTAV research Grant No. 237 (Mexico); the Polish Ministry of Science and Higher Education and the National Science Center; the Ministry of Science and Higher Education of the Russian Federation, Agreement No. 14.W03.31.0026, and the HSE University Basic Research Program, Moscow; University of Tabuk research Grants No. S-0256-1438 and No. S-0280-1439 (Saudi Arabia); Slovenian Research Agency and research Grants No. J1-9124 and No. P1-0135; Agencia Estatal de Investigación, Spain Grant No. RYC2020-029875-I and Generalitat Valenciana, Spain Grant No. CIDE-GENT/2018/020 Ministry of Science and Technology and research Grants No. MOST106-2112-M-002-005-MY3 and No. MOST107-2119-M-002-035-MY3, and the Ministry of Education (Taiwan); Thailand Center of Excellence in Physics; TUBITAK ULAKBIM (Turkey); National Research Foundation of Ukraine, project No. 2020.02/0257, and Ministry of Education and Science of Ukraine; the U.S. National Science Foundation and research Grants No. PHY-1913789 and No. PHY-2111604, and the U.S. Department of Energy and research Awards No. DE-AC06-76RLO1830, No. DE-SC0007983, No. DE-SC0009824, No. DE-SC0009973, No. DE-SC0010007, No. DE-SC0010073, No. DE-SC0010118, No. DE-SC0010504, No. DE-SC0011784, No. DE-SC0012704, No. DE-SC0019230, No. DE-SC0021274, No. DE-SC0022350; and the Vietnam Academy of Science and Technology (VAST) under Grant No. DL0000.05/21-23.

These acknowledgements are not to be interpreted as an endorsement of any statement made by any of our institutes, funding agencies, governments, or their representatives.

We thank the SuperKEKB group for the excellent operation of the accelerator and their special efforts to accomplish this center-of-mass energy scan; the KEK cryogenics group for the efficient operation of the detector solenoid magnet; the KEK computer group and the NII for on-site computing support and SINET6 network support; and the raw-data centers at BNL, DESY, GridKa, IN2P3, INFN, and the University of Victoria for offsite computing support.

-
- [1] N. Brambilla *et al.*, *Eur. Phys. J. C* **71**, 1534 (2011).
 [2] N. Brambilla *et al.*, *Eur. Phys. J. C* **74**, 2981 (2014).
 [3] J. Segovia, P.G. Ortega, D.R. Entem, and F. Fernández, *Phys. Rev. D* **93**, 074027 (2016).
 [4] R.L. Workman *et al.* (Particle Data Group), to be published in *Prog. Theor. Exp. Phys.* **2022**, 083C01 (2022).
 [5] R. Mizuk *et al.* (Belle Collaboration), *J. High Energy Phys.* **10**, 220 (2019).
 [6] X.K. Dong, X.H. Mo, P. Wang, and C.Z. Yuan, *Chin. Phys. C* **44**, 083001 (2020).
 [7] Z.Y. Bai, Y.S. Li, Q. Huang, X. Liu, and T. Matsuki, *Phys. Rev. D* **105**, 074007 (2022).
 [8] Y.S. Li, Z.Y. Bai, Q. Huang, and X. Liu, *Phys. Rev. D* **104**, 034036 (2021).
 [9] Q. Li, M.S. Liu, Q.F. Lü, L.C. Gui, and X.H. Zhong, *Eur. Phys. J. C* **80**, 59 (2020).

- [10] B. Chen, A.L. Zhang, and J. He, Phys. Rev. D **101**, 014020 (2020).
- [11] J.F. Giron and R.F. Lebed, Phys. Rev. D **102**, 014036 (2020).
- [12] V. Kher, R. Chaturvedi, N. Devlani, and A.K. Rai, Eur. Phys. J. Plus **137**, 357 (2022).
- [13] Y.S. Li, Z.Y. Bai, and X. Liu, Phys. Rev. D **105**, 114041 (2022).
- [14] W.H. Liang, N. Ikeno, and E. Oset, Phys. Lett. B **803**, 135340 (2020).
- [15] N.Hüsken, R.E. Mitchell, and E.S. Swanson, Phys. Rev. D **106**, 094013 (2022).
- [16] E.V. Beveren and G. Rupp, Prog. Part. Nucl. Phys. **117**, 103845 (2021).
- [17] J.T. Castellà and E. Passemar, Phys. Rev. D **104**, 034019 (2021).
- [18] N. Brambilla, S. Eidelman, C. Hanhart, A. Nefediev, C.P. Shen, C.E. Thomas, A. Vairo, and C.Z. Yuan, Phys. Rept. **873**, 1 (2020).
- [19] A. Ali, L. Maiani, A.Y. Parkhomenko, and W. Wang, Phys. Lett. B **802**, 135217 (2020).
- [20] P. Bicudo, N. Cardoso, L. Müller, and M. Wagner, Phys. Rev. D **103**, 074507 (2021).
- [21] P. Bicudo, N. Cardoso, L. Müller, and M. Wagner, arXiv:2205.11475.
- [22] Z.G. Wang, Chin. Phys. C **43**, 123102 (2019).
- [23] S.K. Choi *et al.* (Belle Collaboration), Phys. Rev. Lett. **91**, 262001 (2003).
- [24] N.A. Tornqvist, Z. Phys. C **61**, 525 (1994).
- [25] F.K. Guo, C.H. Duque, J. Nieves, and M.P. Valderrama, Phys. Rev. D **88**, 054007 (2013).
- [26] M. Karliner and S. Nussinov, J. High Energy Phys. **07**, 153 (2013).
- [27] Y. Yamaguchi, A. Hosaka, S. Takeuchi, and M. Takizawa, J. Phys. G **47**, 053001 (2020).
- [28] M.T. AlFiky, F. Gabbiani, and A.A. Petrov, Phys. Lett. B **640**, 238 (2006).
- [29] E.S. Swanson, Phys. Rept. **429**, 243 (2006).
- [30] G. Li and W. Wang, Phys. Lett. B **733**, 100 (2014).
- [31] P.G. Ortega, D.R. Entem, and F. Fernández, Symmetry **13**, 1600 (2021).
- [32] F.K. Guo, U.G. Meißner, and W. Wang, Eur. Phys. J. C **74**, 3063 (2014).
- [33] Z.Y. Zhou, D.Y. Chen, and Z.G. Xiao, Phys. Rev. D **99**, 034005 (2019).
- [34] M. Karliner and J.L. Rosner, Phys. Rev. Lett. **115**, 122001 (2015).
- [35] D. Ebert, R.N. Faustov, and V.O. Galkin, Phys. Lett. B **634**, 214 (2006).
- [36] D. Ebert, R.N. Faustov, and V.O. Galkin, Mod. Phys. Lett. A **24**, 567 (2009).
- [37] A. Ali, C. Hambrook, I. Ahmed, and M.J. Aslam, Phys. Lett. B **684**, 28 (2010).
- [38] R.D. Matheus, S. Narison, M. Nielsen, and J.M. Richard, Phys. Rev. D **75**, 014005 (2007).
- [39] S. Chatrchyan *et al.* (CMS Collaboration), Phys. Lett. B **727**, 57 (2013).
- [40] G. Aad *et al.* (ATLAS Collaboration), Phys. Lett. B **740**, 199 (2015).
- [41] X.H. He *et al.* (Belle Collaboration), Phys. Rev. Lett. **113**, 142001 (2014).
- [42] K. Akai, K. Furukawa, and H. Koiso (SuperKEKB Accelerator Team), Nucl. Instr. and Methods Phys. Res. Sect. A **907**, 188 (2018).
- [43] T. Abe *et al.* (Belle II Collaboration), arXiv:1011.0352.
- [44] F. Abudinén *et al.* (Belle II Collaboration), Chin. Phys. C **44**, 021001 (2020).
- [45] D. J. Lange, Nucl. Instr. and Methods Phys. Res. Sect. A **462**, 152 (2001).
- [46] G. Rodrigo, H. Czyż, J.H. Kühn, and M. Szopa, Eur. Phys. J. C **24**, 71 (2002).
- [47] S. Agostinelli *et al.* (GEANT4 Collaboration), Nucl. Instr. and Methods Phys. Res. Sect. A **506**, 250 (2003).
- [48] T. Kuhr, C. Pulvermacher, M. Ritter, T. Hauth, and N. Braun (Belle II framework software group), Comput. Softw. Big Sci. **3**, 1 (2019).
- [49] Y. Iwasaki, B. Cheon, E. Won, X. Gao, L. Macchiarulo, K. Nishimura, and G. Varner, IEEE Trans. Nucl. Sci. **58**, 1807 (2011).
- [50] E. Kou *et al.* (Belle II Collaboration), Prog. Theor. Exp. Phys. **2019**, 123C01 (2019), [Erratum: PTEP **2020**, 029201 (2020)].
- [51] See Supplemental Material at xxxxx (to be added by the publisher), for the two-dimensional distributions of $M(\pi^+\pi^-\pi^0)$ versus $M(\gamma\Upsilon(1S))$ at $\sqrt{s} = 10.701, 10.745$, and 10.805 GeV.
- [52] T. Skwarnicki, Ph.D. thesis, Institute for Nuclear Physics, 1986; DESY Report No. DESY F31-86-02, 1986.
- [53] S.S. Wilks, Ann. Math. Stat. **9**, 60 (1938).
- [54] Y.S. Zhu, Nucl. Instr. and Methods Phys. Res. Sect. A **578**, 322 (2007).
- [55] Please see Sec. 3.2. S. Actis *et al.* (Working Group on Radiative Corrections and Monte Carlo Generators for Low Energies Collaborations), Eur. Phys. J. C **66**, 585 (2010).
- [56] E.A. Kuraev and V.S. Fadin, Yad. Fiz. **41**, 733 (1985) [Sov. J. Nucl. Phys. **41**, 466 (1985)].
- [57] S. Jadach, B.F.L. Ward, and Z. Wąs, Phys. Rev. D **63**, 113009 (2001); Comput. Phys. Commun. **130**, 260 (2000).
- [58] M. Benayoun, S.I. Eidelman, V.N. Ivanchenko, and Z.K. Silagadze, Mod. Phys. Lett. A **14**, 2605 (1999).
- [59] X.Y. Gao, C.P. Shen, and C.Z. Yuan, Phys. Rev. D **95**, 092007 (2017).
- [60] See Supplemental Material at xxxxx (to be added by the publisher), for input values for calculations of the upper limits.
- [61] See Supplemental Material at xxxxx (to be added by the publisher), for individual systematic uncertainties considered in the measurements of $\sigma_B(e^+e^- \rightarrow \omega\chi_{bJ})$ and $\sigma_B(e^+e^- \rightarrow \gamma X_b)\mathcal{B}(X_b \rightarrow \omega\Upsilon(1S))$.
- [62] F. K. Guo, Ulf-G. Meißner, and C. P. Shen, Phys. Lett. B **738**, 172 (2014).
- [63] In Ref. [62], the ratio is given to the $\Upsilon(10860)$ decays under the assumption of D -wave. After discussing with the authors of Ref. [62], such ratio is also applicable for the $\Upsilon(10753)$.